

# Control Strategy for the Discharge Phase of an Ultra-High Voltage ( $>7\text{kV}$ ) Bi-Directional Flyback Converter Driving Capacitive Actuators

Raphaël Mottet, Alexis Boegli, Yves Perriard  
 Integrated Actuators Laboratory (LAI)  
 Ecole polytechnique fédérale de Lausanne (EPFL)  
 Neuchâtel, Switzerland  
 contact: raphael.mottet@epfl.ch

**Abstract**—Dielectric Elastomer Actuators (DEAs) require ultra high voltages in the order of several kilo volts to operate. To supply such voltages, a DC-DC flyback converter topology was selected. One of the main advantage of using such a structure is the possibility to modify it to work bi-directionally. Meaning that electrical energy can not only flow from the power supply to the actuator, but also from the actuator back to the power supply. This characteristic is of significant importance because of the need to recuperate the electrical energy stored in DEAs to improve the overall efficiency of the system instead of dissipating it as heat. Indeed, due to their capacitive nature, DEAs can store an important amount of energy when fully deformed which needs to be removed to bring the actuator back to its original shape.

This paper focuses on the control aspect to remove the stored energy when using a bi-directional flyback converter capable to supply a voltage of up to  $7\text{kV}$  to the load from a  $12\text{V}$  power supply.

After a brief presentation of the working principle of the discharge procedure, the implemented control strategy is detailed in depth with the presentation of the hardware used and the control algorithm put in place.

Experimental results then show that the control strategy works well with an output voltage of up to  $7\text{kV}$  but is nonetheless close to its limits because of increasingly small measuring time spans going down to several micro seconds.

**Index Terms**—dielectric elastomer actuators, flyback converter, ultra-high voltage gain, high voltage power supply, discharge control

## I. INTRODUCTION

The interest to use Dielectric Elastomer Actuators (DEAs) in portable or embedded applications due to their advantageous characteristics (e.g. lightness, high flexibility and large displacements [1][2]) has been increasing over the past few decades. However, while working with this technology one will face several major challenges, one of which is the necessity to be able to manipulate high voltages that can reach up to several thousands of volts.

This need originates from the way DEAs are manufactured and how they operate. Indeed, a basic DEA consists of a flexible dielectric layer sandwiched between two compliant electrodes effectively creating a flexible capacitor [3] and motion happens when a voltage high

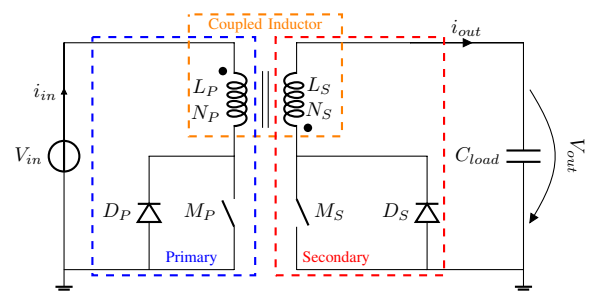


Fig. 1. Basic schematic of a bi-directional DC-DC flyback converter.  $L_P$  is the primary and  $L_S$  the secondary inductance combined as a coupled inductor (orange) of  $N_P$  and  $N_S$  turns respectively.  $C_{load}$  represents an ideal Dielectric Elastomer Actuator.

enough is applied across the electrodes such that the electrostatic force brings them towards one another. The electrodes thus compress the dielectric layer vertically which will then expand laterally.

To maximize the compression and resulting lateral expansion, one must try to work close to the electrical breakdown limit of the dielectric layer which is typically of about  $5\text{kV}$ ,  $10\text{kV}$  or  $20\text{kV}$  and is proportional to the layer thickness. While using with the thinnest thickness allows to work with lower voltages, the DEA manufacturing process becomes significantly more complex [4].

Therefore, to generate and manipulate the necessary voltages, the bi-directional flyback converter structure (Fig.1) was selected as it not only possesses the ability to amplify a low input voltage to several thousands of volts but can also recuperate a portion of the energy stored in the load as was done by Thummala in [5] where he amplified an input voltage of  $24\text{V}$  to  $2.5\text{kV}$  across a capacitive load and subsequently recovered parts of the energy stored.

Nevertheless, as mentioned above, these output voltage levels are not high enough for conventional DEAs. Thus, with the goal to overcome this problem, a study was undertaken in [6] to determine what limits the ability of the structure to supply voltages over  $2.5\text{kV}$  and it was revealed that a major limiting factor were the parasitic capacitances found throughout the converter.

However, more specifically for bi-directional flyback converter, an additional significant limiting factor is the secondary switch which enables the bi-directional behav-

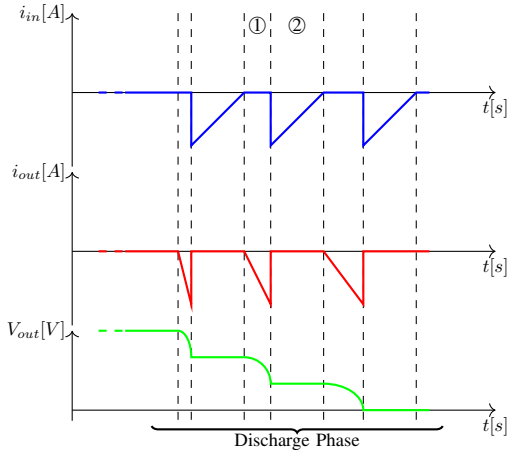


Fig. 2. Ideal input current  $i_{in}$ , output current  $i_{out}$  and output voltage  $V_{out}$  in a bi-directional flyback converter during the discharge phase. During the period ① the switch  $M_S$  is closed and during ②  $M_S$  is open. The slope of  $i_{out}$  varies because of the rise and following drop of  $V_{out}$ .

ior. A first challenge regarding this switch is that MOSFETs capable to withstand the ultra-high voltages targeted (5 kV and more) are nonexistent as the best ones commercially available have a breakdown voltage of 4.5 kV. To overcome this challenge, several 4.5 kV MOSFETs can be put in series using the Pulsed Transformer Gated Drive (PTGD) topology as explained in detail in [7] and, in our case for this publication, a PTGD switch made of two of such MOSFETs (effectively creating a 9 kV switch) was successfully integrated into a bi-directional flyback capable to amplify an input voltage of 12 V to 7 kV was manufactured.

The second challenge and main discussion point of this publication concerns the control of said PTGD switch. Indeed, with the bi-directional flyback converter supplying higher and higher output voltages, the duration during which the PTGD switch must remain closed decreases because of said output voltage across the load as is explained further below and can become extremely short in the order of a few microseconds. Consequently, the strategy used to dynamically change this time interval is critical for the proper operation of the converter.

This publication will first explain the basic working principles of the flyback which concern the PTGD switch. Then, a solution for the control of said switch will be presented and implemented. This solution includes a simple electronic circuit that allows the use of the ultra-fast Analog-to-Digital Converter (ADC) module of a microcontroller to measure the output current as well as an algorithm to use the measured current values to determine the best time reopen the switch. Finally, the performances of this subsystem are presented and discussed.

## II. BI-DIRECTIONAL FLYBACK : DISCHARGE PHASE WORKING PRINCIPLE

The basic working principle of a unidirectional flyback converter essentially consists of transmitting pulses of energy from a DC power supply to a load through a

TABLE I  
CHARACTERISTICS OF THE 7kV FLYBACK'S COUPLED INDUCTOR

Parameter	Value
Material	Ferrite N87
Geometry	RM14
Air gap	0.15 mm
Max energy stored $\mathcal{E}_{mag,max}$	6.3 mJ
Winding method	Segmented Discontinuous Side-by-side
Primary number of segments	1
Primary number of turns $N_P$	18
Primary inductance $L_P$	240.5 $\mu$ H
Primary leakage inductance $L_{LP}$	19.7 $\mu$ H
Primary winding capacitance $C_P$	8.6 nF
Primary winding resistance $R_P$	281 m $\Omega$
Secondary number of segments	3
Secondary number of turns $N_S$	720
Secondary inductance $L_S$	420.9 mH
Secondary leakage inductance $L_{LS}$	34.7 mH
Secondary winding capacitance $C_S$	5.8 pF
Secondary winding resistance $R_S$	111.5 $\Omega$
Inter-winding capacitance $C_W$	12.5 pF

coupled inductor by controlling the primary switch  $M_P$ . In the case of a capacitive load, this process makes the output voltage  $V_{out}$  gradually increase and it is known as the charge phase.

By adding a secondary switch  $M_S$  the bi-directional nature of the flyback topology is enabled. Meaning that, once the targeted output voltage is reached across the load, activating  $M_S$  in a similar fashion as  $M_P$  during the charge phase the energy stored in the load will be gradually removed and sent back towards the power supply thus reducing the output voltage as shown in Fig. 2.

The main difference between the charge and discharge phases is the fact that the voltage dictating the time it takes for the coupled inductor to be filled with energy is first constant during the charge phase ( $V_{in}$  is constant) and then varies during the discharge phase ( $V_{out}$  decreases with each pulse). This time can be estimated for each pulse with

$$t_{on} = \frac{L}{U}i \quad (1)$$

where  $t_{on}$  is the time during which the relevant switch is closed,  $L$  is the primary or secondary inductance of the coupled inductor during the charge and discharge phase respectively,  $U$  is the voltage applied across the inductance  $L$  and  $i$  is the peak current value flowing through the inductance  $L$ .

It is critical to be able to master as precisely as possible  $t_{on}$  because if either switches are left closed for too long during their respective phases, the core of the coupled inductor will saturate which will allow the current flowing through to rise out of control leading to avoidable energy losses or in the worst case to the destruction of the electronics.

To give a concrete example of how fast the secondary switch must be controlled at high voltages, let us consider a custom made coupled inductor which characteristics

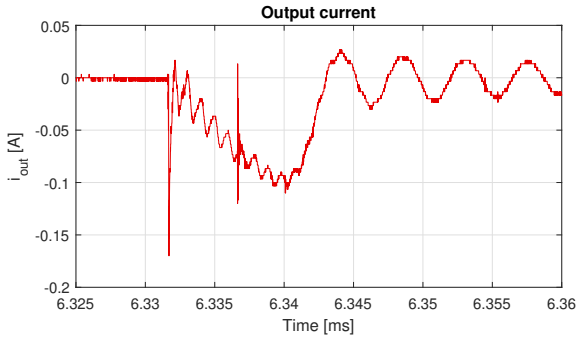


Fig. 3. Output current during the discharge phase with an output voltage of 7 kV across the capacitive load. The current reaches 0.1 A in approximately 7  $\mu$ s.

can be found in Table I. With the inductance value, the geometry and the material used, one can calculate that the peak  $i_{out}$  current for which the core starts to saturate is of around 160 mA. To avoid the risk of crossing that threshold, let us consider a current value of 100 mA. By using this value in (1) as well as the values of the secondary inductances  $L_S$  and  $L_{LS}$ , and an output voltage of 7 kV,  $t_{on}$  is equal to 6.5  $\mu$ s as is approximately the case in the measure shown in Fig. 3.

### III. ADC BASED CONTROL STRATEGY FOR THE DISCHARGE PHASE

To make sure that the current flowing through the coupled inductor during the discharge does not exceed the saturation current of the core, it is necessary to implement a control strategy that dynamically adapts the  $t_{on}$  duration of the secondary switch as the output voltage drops during the discharge phase.

#### A. Hardware Implementation

To do so, the selected solution that was implemented in the 7 kV bi-directional flyback and which is presented here makes use of the fast ADC module of TI's TMS320F28379D microcontroller to measure the output current. This module is capable to operate at up to 3.5 MSPS with a 12 bits resolution and single ended inputs. The high frequency capability is necessary to make enough measurements during the  $t_{on}$  time span to quickly and reliably make sure that  $i_{out}$  does not exceed the set security threshold.

To measure the current  $i_{out}$  which flows through the capacitive load, a 10  $\Omega$  shunt resistor was used. However,  $i_{out}$  generates a negative voltage across the shunt resistor which means that the resulting voltage cannot be directly fed into the ADC as only single ended inputs can be read. To overcome this, a voltage follower inverting operational amplifier was added to the system as shown in Fig. 4.

#### B. Software Implementation

Regarding the software implementation, the algorithm works as follows and Fig. 5 gives a visual representation of the various timings of the interrupts :

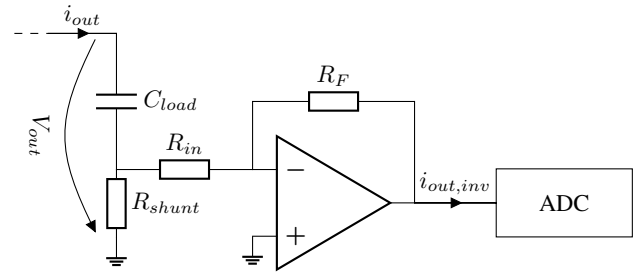


Fig. 4. Circuit inverting the measured signal  $i_{out}$  to make it readable by the ADC of the microcontroller. Here,  $C_{load} = 2.4$  nF,  $R_{shunt} = 10 \Omega$ .  $R_1$  and  $R_2$  are identical and are 1 k $\Omega$  resistors.

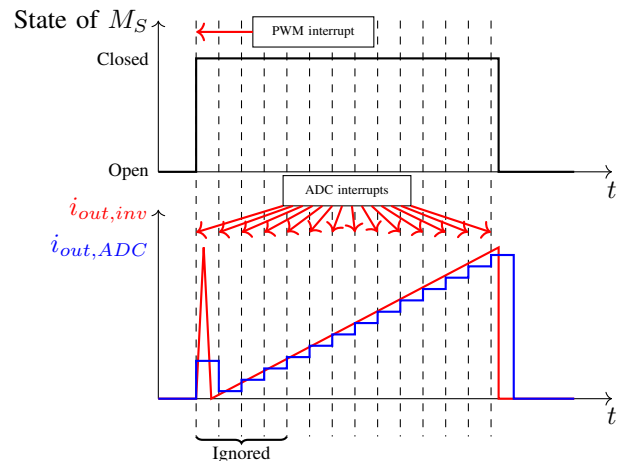


Fig. 5. Visual representation of the various occurrences of the interrupts for the operation of the secondary switch during the discharge phase.

- 1) When the command to discharge the load is sent, the PWM timer linked to the PTGD switch is enabled.
- 2) When the PWM counter passes a set compare value, the polarity of the control pin is set to high to close the switch and an interrupt is triggered.
- 3) This interrupt enables the ADC timer which is set to a sampling frequency of 2.8 MSPS to read the voltage coming out of the inverting operational amplifier. Each reading triggers an interrupt during which the measured value is compared to a manually fixed threshold value. The first 5 measurements are however ignored because of the large initial voltage spike visible in Fig. 3 due to the closing of the switch as it would cause a false positive to trigger the reopening of the switch.
- 4) Once the threshold value is reached or exceeded, the ADC timer is disabled and reset. The counter of the PWM is also set back to 0 which forces the polarity of the control pin to be set back to low, effectively telling the switch to reopen.

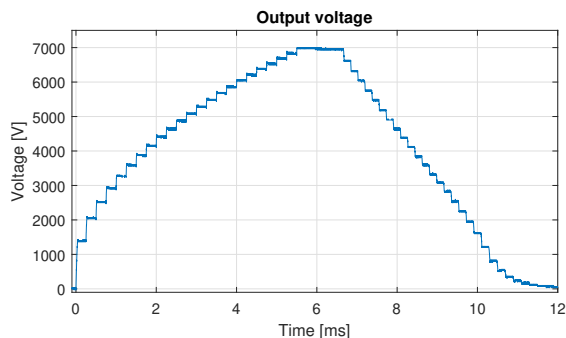


Fig. 6. Output voltage across the capacitive load. Thanks to the constant pulses of energy during the charge and discharge phases, the voltage rises and falls nearly symmetrically.

- 5) In the case where the output voltage has nearly reached 0 V and the current cannot rise above the threshold value due to the low amount of energy left in the load, the switch is automatically reopened after a set amount of time. This security is absolutely necessary because of how the PTGD works. As explained in [7], this time duration depends of the characteristics of the transformer of the switch and how long it will take to reach saturation.

#### IV. EXPERIMENTAL RESULTS

By implementing the control strategy presented above, it is now possible to reliably operate the secondary 9 kV PTGD switch of the bi-directional flyback converter in such a way that the amount of energy removed from the capacitive load is controlled and, in this case, constant. This leads to a smooth and symmetrical charge and discharge cycle even with a high output voltage of 7 kV as shown in Fig. 6.

As for the output current, Fig. 7 and 8 show the actual negative current measured through a  $10\Omega$  shunt resistor, the current waveform after the inverting circuit and finally the current measured by the ADC module during the first pulse of the discharge phase when the output voltage is of 7 kV and then when the output voltage is much lower around 1.2 kV.

The aforementioned figures show that the control strategy works well and can reliably operate the bi-directional flyback at ultra-high voltage levels. However, Fig. 7 reveals several noticeable aspects that may need to be considered for future iterations.

First, at high voltage, the implemented strategy is close to the limit of what it is capable of as the sampling frequency is near the maximum available; the duration during which it must take measurements is extremely short; and the current during the first few microseconds is very noisy. Consequently, if the voltage increases further and the time span shortens, the measured current may end up being heavily dominated by noise which could in turn be falsely interpreted by the control system to reopen the switch.

Second, there is a delay of a few microseconds between the moment the switch is ordered to reopen and

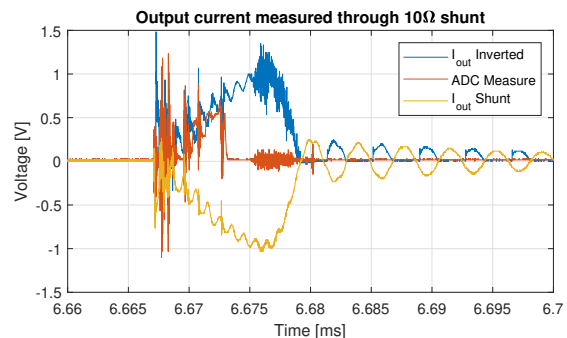


Fig. 7. Measured waveforms of the output current made when the output voltage is of 7 kV. Once directly on the  $10\Omega$  shunt, once after the inverting circuit and finally the actual measured values obtained with the ADC (shown by putting them out through a Digital-to-Analog Converter).

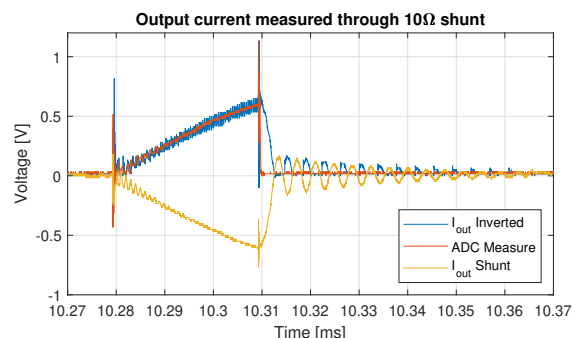


Fig. 8. Measured waveforms of the output current made when the output voltage is of 1.2 kV. Once directly on the  $10\Omega$  shunt, once after the inverting circuit and finally the actual measured values obtained with the ADC.

the moment it actually starts opening. Meaning that, to make sure that the current does not saturate the core, the threshold value in the code must include a large safety margin compared to what may be calculated with (1).

And finally, the switch is slow to reopen as shown by the significant amount of time it take for the current to fall back down to 0 A. This aspect originates from the way the PTGD topology works and thus means that further work should be done to find way to accelerate the opening of the switch. Doing so would greatly help reduce the resulting commutation losses during the reopening period.

In Fig. 8, one can see the security procedure in effect where after a set amount of time (here  $30\mu\text{s}$ ) the switch reopens regardless if the current reached the maximal tolerated peak value. This security must be implemented as the PTGD cannot be left open for longer than the amount of time it takes for the PTGD transformer to reach saturation.

#### V. CONCLUSION

This paper proposes a control strategy and the necessary electronics used to operate the secondary switch of an ultra-high voltage bi-directional flyback converter. The control system was tested on a bi-directional flyback capable to supply up to 7 kV to a capacitive load and it showed excellent results up to this voltage level. Indeed, the microcontroller managed to adequately operate

a 9 kV Pulsed Transformer Gated Drive switch made out of two 4.5 kV MOSFETs put in series to recuperate the energy stored in a capacitive load charged to 7 kV while dynamically adapting the frequency and duty cycle of the PWM. This allowed to ensure the removal of a constant amount of energy during each commutation and avoid the saturation of the flyback's coupled inductor.

Nevertheless, the analysis of the output current during the discharge phase revealed some of the limitations of that system and strategy. First, because the amount of time it takes for the current to bring the core of the coupled inductor to saturation when the output voltage is high is in the order of the microsecond, the ADC used must be able to work at frequencies in the order of the megahertz so as to measure said current quickly enough to avoid exceeding the saturation threshold as it can lead to the destruction of components. This can result in a large amount of power consumption not ideal for embedded applications.

Second, when the output voltage is high, there is a noticeable delay between the moment the switch is ordered to reopen and the actual reopening. This means that the current continues to flow for a short while before it starts to drop back down to 0 A. This must be taken into account when setting the threshold value in the software.

And finally, the noise and initial current spike that appear when the switch closes increase significantly with the output voltage. Consequently, this control strategy may not be able to properly detect when the current exceeds the threshold in fewer than  $\sim 5 \mu\text{s}$  (i.e. for larger voltages) as the signal would be drowned in noise.

To overcome these limitations, a control strategy involving a different combination of analog and digital electronic should be considered. A potential solution may make use of comparators such as Schmitt triggers to determine when the output current reaches the set threshold. Such a solution could allow the system to react faster and be more precise with its measurements.

#### REFERENCES

- [1] R. D. Kornbluh et al. "Electroelastomers: applications of dielectric elastomer transducers for actuation, generation, and smart structures". In: *Smart Structures and Materials 2002: Industrial and Commercial Applications of Smart Structures Technologies*. Vol. 4698. International Society for Optics and Photonics, July 2002, pp. 254–270.
- [2] Q. Pei et al. "Multifunctional electroelastomer rolls and their application for biomimetic walking robots". In: *Smart Structures and Materials 2002: Industrial and Commercial Applications of Smart Structures Technologies*. Vol. 4698. International Society for Optics and Photonics, July 2002, pp. 246–253.
- [3] Z. Suo. "Theory of dielectric elastomers". en. In: *Acta Mechanica Sinica* 23.6 (Dec. 2010), pp. 549–578.
- [4] M. Almanza et al. "Towards the material limit and field concentration smoothing in multilayer dielectric elastomer actuators". In: *Smart Materials and Structures* 29.4 (2020), p. 045044.
- [5] P. Thummala et al. "Digital Control of a High-Voltage (2.5 kV) Bidirectional DC-DC Flyback Converter for Driving a Capacitive Incremental Actuator". In: *IEEE Transactions on Power Electronics* 31.12 (Dec. 2016), pp. 8500–8516.
- [6] R. Mottet et al. "Critical Parasitic Elements of Coupled Inductors for Ultra-High Voltage Flyback Converters Used to Drive Capacitive Actuators". In: *2019 22nd International Conference on Electrical Machines and Systems (ICEMS)*. Aug. 2019, pp. 1–5.
- [7] Lucas Pniak et al. "Ultra High Voltage Switch for Bidirectional DC-DC Converter Driving Dielectric Elastomer Actuator". In: *IEEE Transactions on Power Electronics* (2020).